Materials Advances

ROYAL SOCIETY OF CHEMISTRY

PAPER

View Article Online
View Journal | View Issue

Cite this: *Mater. Adv.*, 2024, **5**, 7432

Ionogel impregnated glass ionomer cement and the effect of nanoparticle additives†

Sreejith Sasidharan Lathikumari and Manju Saraswathy *

This study focused on improving the mechanical properties of glass ionomer cement (GIC) by incorporating ionic liquid-based nanogel additives called ionogels. Ionogels were synthesized using the ionic liquid, 3,3′-(butane-1,4-diyl)bis(1-vinyl-1*H*-imidazol-3-ium) bromide and a crosslinker, ethylene glycol dimethacrylate *via* free radical solution polymerization. The size of the ionogels was controlled by adding a high concentration of chain transfer agent (20 mol%) and using a solvent-to-monomer ratio of 4 : 1. Modified glass ionomer cements were prepared by incorporating ionogels into polyalkenoic acid formulations at different weight ratios followed by mixing with calcium fluoroalumino silicate glass powder. Additives such as L-tartaric acid and MgO nanoparticles with ionogels were evaluated for the working time, setting time, and mechanical properties of the corresponding GIC. Ionogel incorporation enhanced the compressive strength of the GIC up to 2 weight percentage (wt%). The data show that one wt% titanium hydroxide nanoparticles with one wt% ionogel improved the compressive strength of the glass ionomer cement to 128.70 MPa. The biocompatibility evaluations of the ionogel-modified glass ionomer cement were confirmed according to ISO 10993-5. Intraperitoneal injection of saline and cotton seed oil extract of ionogel-impregnated GIC showed normal behaviour. Consistent body weights were maintained during the experimental period, confirming that ionogel-impregnated GIC is safe to use.

Received 7th June 2024,
Accepted 15th August 2024

DOI: 10.1039/d4ma00592a

rsc.li/materials-advances

1. Introduction

Dental restorations are necessary for restoring lost or damaged teeth with several benefits, including improved social life, appearance, and oral health. Dental restorative materials include amalgam, resin composites, and glass ionomer cement (GIC). The modern scientific community always tries to closely mimic the natural translucency, color, and strength of dental restorative materials, which results in aesthetically pleasing outcomes with improved properties that reduce the risks of many adverse effects of dental materials. However, dental restorative materials available in the market have many limitations. For example, the property of amalgam filling to expand and contract with heat and cold eventually leads to tooth fracture.[1] On the other hand, resin-composite restoration has excellent physical and aesthetic properties. However, the polymerization shrinkage associated with resin composites could cause micro-cracks between the tooth and the restoration, leading to secondary caries.[2]

GIC is an aqueous-based cement formed by an acid–base reaction between the fluoroaluminosilicate glass powder and polyalkenoic acid.[3] GIC has many advantages over other dental restorative materials, including solid adhesion to both enamel and dentin without the need for a coupling agent or etching techniques, anti-cariogenic properties due to the release of fluoride, thermal compatibility with tooth enamel, and better biocompatibility compared to other classes of dental materials.[4–6] In addition to unique physicochemical characteristics, GIC can favor remineralization, increase enamel and dentine resistance to demineralization, and prevent secondary lesions. However, conventional GIC has many disadvantages, including inferior mechanical properties, brittleness, low abrasion resistance, inadequate surface properties, and sensitivity to moisture in the oral cavity when newly placed.[7] GICs have fewer aesthetic options as they tend to have an opaque appearance and may not blend smoothly with the natural tooth colour. Sensitivity towards moisture in the oral cavity during the setting process, which can affect the optimal performance, is also a significant drawback of GIC.[8,9] All these characteristics restrict the use of GIC for many clinical applications.

Many efforts to improve the properties of conventional GIC have been reported.[10] The critical modification in these aspects is resin-modified GIC (RMGIC).[11] Different additives to improve the physicochemical properties of GIC, including mechanical

Division of Dental Products, Department of Biomaterial Science and Technology, Biomedical Technology Wing, Sree Chitra Tirunal Institute for Medical Sciences and Technology, Thiruvananthapuram, 695012, India. E-mail: manjus@sctimst.ac.in; Tel: +91-471-2520441, +91-9539263017

† Electronic supplementary information (ESI) available. See DOI: https://doi.org/10.1039/d4ma00592a

properties,[12,13] viscosity,[14] flow ability,[15] working time, and setting time of GIC, have been reported.[16,17] Additives, including titanium oxide nanoparticles,[18,19] zinc oxide,[20,21] hydroxyapatite,[22–24] and zirconium oxide,[25,26] have been tried for various property improvements. The addition of polymer powder (*e.g.*, gum Arabic powder) to improve the mechanical properties of glass ionomer cement was also established by many researchers.[27] Studies on antimicrobial agents such as metal nanoparticles and bioactive agents can reduce the risk of secondary caries, biofilm formation, and other oral infections.[28,29]

Many studies have demonstrated that not all the carboxyl groups of polyalkenoic acid were converted to carboxylate groups during the reaction with glass powder.[30,31] The high possibility of inter or intramolecular hydrogen bonding in polyalkenoic acid leads to a rigid polymer matrix. It causes steric hindrance and limits the formation of salt bridges, which reduces the proper interaction of polyalkenoic acid with glass powder during acid–base reaction, eventually leading to reduced mechanical properties.[32] Polyalkenoic acid modification reduces the inter/intramolecular hydrogen bonding. It improves the flexibility within the polymer matrix, thereby increasing the availability of functional groups in polyalkenoic acid that interact with glass powder. However, studies on polyalkenoic acid modification to improve the mechanical properties of glass ionomer cement are restricted to the copolymerization of polyacrylic acid using monomers such as itaconic acid, maleic acid, *etc.* The use of additives that can reduce the inter or intramolecular hydrogen bonding within the polyalkenoic acid formulation is a better alternative.

Nanogels are three-dimensional polymer networks ranging from 100 to 500 nm.[33–35] They were synthesized by free radical solution polymerization. It was reported that nanogel additives in dental restorative materials could enhance compressive strength, hardness, wear resistance, and durability.[36,37] In addition, the nanogel could play a key role in reducing the shrinkage stress and volumetric shrinkage that occurred during the curing of the resin in the composites. Efficient distribution of stress and load-bearing capacity of the nanostructured gel form has also been reported elsewhere.[38–43] However, the application of nanogels to improve the physicochemical properties of GIC is not explored so far. Nanogels can be a potential additive to GIC, which can interfere with the formation of inter/intra molecular hydrogen bonding between polymer chains in polyalkenoic acid formulations, retaining the flexibility of the polymer chain and enhancing salt bridge formation. The ionic content in the nanogel may alter the interaction between polyalkenoate and the glass powder. The present study integrates an ionic liquid into a nanogel framework. The ionic liquid-based nanogels called ionogels were incorporated into glass ionomer cement, and the impact on the mixing compatibility, mechanical properties, and biocompatibility of GIC were measured. To the best of our knowledge, no such study has been reported on ionogel-incorporated GIC. This study aims to deliver valuable insight into the viability of ionogel-incorporated GIC to the scientific community and to demonstrate a new strategy to enhance the mechanical properties and biocompatibility of GIC.

1.1 Materials

Acrylic acid (99%), ammonium persulfate (APS), itaconic acid (99%), 1-Vinyl-2-pyrrolidone (≥99.0%), aluminum fluoride trihydrate (97%), ammonium trihydrate (97%), sodium hexafluoroaluminate (97%), sand or white quartz, aluminum oxide activated neutral, aluminum phosphate, strontium fluoride, 1-vinyl imidazole (≥99%), 1,4-dibromo butane (99%), 2-propanol, hydroxyapatite (≥97.0%), zirconium(IV)oxide (99%, 5 μm), titanium(IV)oxide (≥99.5%, 21 nm), and 2,2′-azobis(2-methylpropionitrile) (AIBN) (99%) were purchased from Sigma-Aldrich, Bangalore, India. Toluene (99%), diethyl ether (99%) and 2-mercaptoethanol (99%) were purchased from SiSCO Research Laboratories Pvt. Ltd, Mumbai, India. All other reagents were of analytical grade and used as such without any further purification.

1.2 Synthesis of polyalkenoic acid

Polyalkenoic acid was synthesized *via* copolymerization of acrylic acid, itaconic acid and vinyl pyrrolidone at a molar ratio of 8 : 1 : 1. Briefly,[44] 0.346 mol of acrylic acid was added to the three-necked flask and diluted with distilled water. Then 2 wt% of APS (2.54 mmol) and 20 mol% of isopropanol were added to the above solution. The reaction mixture was refluxed at 300 rpm and 85 °C for 6 h and 0.0436 mol of itaconic acid and 0.0436 mol of vinyl pyrrolidone in water were added along with 2 wt% APS (4.719 mmol). After the reaction, the reaction mixture was concentrated using a rotary evaporator. The concentrated samples were freeze-dried and stored in a refrigerator. Half of the purified copolymer, poly(AA-*co*-IA-*co*-VP), was dissolved in distilled water to prepare a 45% polyalkenoic acid solution and stored in an amber-colour plastic bottle for GIC preparation. The second portion of poly(AA-*co*-IA-*co*-VP) powder was used for physicochemical characterization.

1.3 Preparation of glass powder

Fluoroalumino silicate glass powder was synthesized *via* a multistep process started with the preparation of the fusing mixture. The composition of the fusing mixture is detailed in Table T1 (ESI†). The fusing mixture in acetone was mixed thoroughly with a mortar and pestle and dried in a hot air oven at around 80 °C. The dried samples were weighed in a platinum crucible and placed in an electric furnace at 1250 °C for 2.5–3 h. The molten glass was quenched in normal water. Glass particles were separated from the platinum crucible and pulverized in a ball mill using 20 mm and 10 mm balls at 60 rpm for 3 h each. The pulverized glass particles were collected and sieved through 44 μm mesh sieves and stored at room temperature.

1.4 Ionogel synthesis

Ionogel was synthesized *via* a two-step reaction. In the first step, an ionic liquid was prepared as reported earlier.[45] The ionic liquid, 3,3′-(butane-1,4-diyl)bis(1-vinyl-1*H*-imidazol-3-ium) bromide, as a precursor of the nanogel was prepared *via* the addition of di-bromobutane into 1-vinyl imidazole under a blanket

of nitrogen. After 48 h, the reaction mixture was precipitated in diethyl ether. A white crystalline salt of imidazolium was formed. The supernatant was decanted and the crystals were dissolved in methanol. The mixture was precipitated with diethyl ether. The structure of ionic liquid (3,3′-(butane-1,4-diyl)bis(1-vinyl-1*H*-imidazol-3-ium) bromide) was characterized using FTIR, and ^{1}H NMR. In the second step, an ionogel was synthesized as reported elsewhere with slight modifications.[45–47] Briefly, the ionogel was synthesized using 3,3′-(butane-1,4-diyl)bis(1-vinyl-1*H*-imidazol-3-ium) bromide and ethylene glycol dimethacrylate at 80 : 20 molar ratio *via* free radical solution polymerization. A three-necked round bottom flask was added with 28 mL methanol and 2 g of 1,4-di(vinyl imidazolium) butane bis bromide (4.9487 mmol). Ethylene glycol dimethacrylate (1.237 mmol, 0.24 g), 0.0224 g AIBN and 0.1079 mL mercaptoethanol were added to the reaction mixture while stirring. The reaction mixture was stirred continuously for 2.5 h at 300 rpm, 85 °C and precipitated in diethyl ether. The ionogel settled in the bottom layer and was collected and dried in a vacuum oven.

1.5 Residual monomer content estimation

High-pressure liquid chromatography was used to determine the residual monomer content of the polyalkenoic acid solution (1 mg mL^{-1} in DI water). Briefly, 20 μL of polyalkenoic acid solution was injected into the column and the sample was separated using acetonitrile/0.1% phosphoric acid solution (90%) at a flow rate of 0.6 mL min^{-1} and column temperature at 30 °C. The chromatogram was recorded with a UV detector at 210 nm wavelength. Calibration curves were constructed using standard solutions of acrylic acid, itaconic acid, and *N*-vinyl pyrrolidone at different concentrations (say, 500 μg mL^{-1}, 250 μg mL^{-1}, 125 μg mL^{-1}, 62.5 μg mL^{-1}, and 31.25 μg mL^{-1}) separately by plotting the peak area against the concentration. The solution was analyzed in triplicate. The unknown concentration of the extract was calculated using the calibration curve.

1.6 Preparation of glass ionomer cement

Polyalkenoic acid incorporated with 15% tartaric acid acts as a setting modifier. The liquid-to-powder ratio was fixed at 2.7; which means that for every 100 mg of liquid used, 270 mg of powder was incorporated and prepared the cement. During mixing, the glass powder was divided into two portions, one portion was slowly mixed with 45% polyalkenoic acid using a plastic spatula and the remaining portion was incorporated into the premixed portion.

1.7 Fourier transform infrared spectroscopy

The absence of residual monomers in polyalkenoic acid formulation was analysed using Fourier transform infrared spectroscopy (Shimadzu IR Spirit in ATR mode). The transmission spectra were collected in the range of 4000–400 cm^{-1} by placing a thin uniform layer of sample perpendicular to the infrared radiation path.

1.8 Gel permeation chromatography (GPC)

The molecular weight of the polyalkenoic acid was calculated using Gel permeation chromatography (Waters HPLC/GPC system with 600 E Series Pump and 7725 Rheodyne Injector). The ultra hydrogel linear column was used as a stationary phase and a buffer solution containing 0.25 $NaNO_3$ and 0.01 M NaH_2PO_4 was used as the mobile phase at a flow rate of 1 mL min^{-1}. A refractive index detector (Waters 2414) was used to analyze the sample. A known amount of the sample was weighed and dissolved in 1 mL of deionized water and 20 μL of the sample solution was injected into the chromatographic system for analysis.

1.9 Thermogravimetric analysis (TGA)

Thermogravimetric analysis (TGA) was done in SDT Q 600 (TA Instruments, USA) to determine the thermal stability of the polyalkenoic acid. 10–12 mg of the sample was taken in a platinum cup and heated under a nitrogen atmosphere at the heating rate of 10 °C min^{-1} from room temperature (R.T.) to 800 °C. The procedure used for TGA analysis was based on the standard ASTM-E-1131-07 (2007).

1.10 Differential scanning calorimetry

Differential scanning calorimetry (DSC) of the sample was carried out using Q100 (TA instruments, USA). 5 mg of the sample was taken in a hermetic aluminum pan and heated to 100 °C and cooled back at the rate of 1 °C min^{-1} in an atmosphere of nitrogen. The procedure was based on ASTM E537-07 (2007).

1.11 Nuclear magnetic resonance spectroscopy (NMR)

^{1}H nuclear magnetic resonance spectra of the sample in deuterated water at 300 K were recorded using a Bruker Avance Spectrometer (500 MHz). Tetra methyl silane (TMS) was used as the internal standard.

1.12 Dynamic light scattering

The particle size of the ionogel was measured using a Zetasizer Nano analyzer (ZS, Malvern instrument Ltd Worcestershire, UK) using the dynamic light scattering technique.

1.13 Scanning electron microscopy (SEM)

The surface morphology and size of the glass powder were measured using scanning electron microscopy (Model S2400, Hitachi). The samples were imaged at an accelerating voltage of 15 kV and a working distance of 10 cm.

1.14 Working and setting time

Powder and polyalkenoic acid solution (liquid) was weighed into a small glass plate according to the P/L (powder/liquid) ratio. The glass powder was mixed into a polyalkenoic acid solution using a plastic spatula. Working time was denoted as the time when the material could no longer cohesively string to a small height when lifted with a spatula. Initial setting time was determined as the point at which no permanent indentation in the material is possible with a certain force using the spatula. The experimental testing was conducted at (24 ± 1 °C).

1.15 Mechanical properties

The mechanical testing of GIC was carried out using an Instron 3365. A 5 kN load cell was used to measure both compressive strength and diametrical tensile strength with the crosshead speed of 0.75 mm min^{-1} for compressive strength and 0.5 mm min^{-1} for diametrical tensile strength. The mechanical test was measured at 26 °C and a relative humidity of ~60%.

1.15.1 Compressive strength. Cylindrical specimens of height 6.0 ± 0.1 mm and diameter 4.0 ± 0.1 mm were made in a PTFE mould and tested for compressive strength. The mould was filled with the material and covered with a thick plastic sheet on both sides, flattened under load using a hydraulic press and stored at 24 °C for 10 min. Samples were collected and immersed in distilled water (DI water) for 24 h in a small 5 mL glass vial at 37 °C. Samples were removed from DI water and dried in the oven at 37 °C. Six identical specimens were used for each experiment.[48,49]

1.15.2 Diametrical tensile strength. The samples were prepared using a PTFE mould of 6 mm diameter and 4 mm thickness. The powder and liquid composition of GIC was mixed at a specific powder/liquid (P/L) ratio using a plastic spatula. The cement was filled in the mould immediately after reaching the working time. The mould was filled with the GIC and flattened under a load using a hydraulic press at 24 °C for 10 min. Samples were immersed in DI water for 24 h in a small 5 mL vial at 37 °C. After 24 h, samples were removed from water and dried in an oven at 37 °C and the diametrical tensile strength was measured. Six identical specimens were used for each experiment.[48,49]

1.16 Radiopacity

Samples with dimensions 6 mm diameter × 4 mm thickness were prepared using a PTFE mold, (6 mm × 4 mm). The samples were irradiated with X-rays. The thicknesses of aluminium step wedge ranging from 0.5 to 5 mm were used as controls.

1.17 *In vitro* cytotoxicity

In vitro cytotoxicity tests for the conventional glass ionomer cement (GNG0) and titanium oxide nanoparticle-modified ionogel-impregnated glass ionomer cement (TiGNG1) were performed using the direct contact method as per ISO 10993-5, 2009.[50,51] Ultra-high molecular weight polyethylene was used as the negative control and stabilized PVC disc was used as the positive control. The test samples were sterilized by ethylene oxide. L929 mouse fibroblast cells were incubated with the negative control, positive control, GNG0 and TiGNG1 in triplicate at 37 ± 1 °C for 24 to 26 h. After incubation, the cell monolayer was examined microscopically for the response around the test samples.

1.18 *In vivo* acute systemic toxicity

1.18.1 Acute intraperitoneal application of cotton seed oil extract of TiGNG1 in Swiss albino mice. The systemic response of Swiss Albino mice following intraperitoneal injection of cotton seed oil extract of the titanium oxide nanoparticle-modified ionogel-impregnated glass ionomer cement (TiGNG1) was evaluated. All animal experiments were performed in compliance with the Institutional Animal Ethics Committee (No. SCT/IAEC-346/May/2020/105). The study was conducted as per the standard, ISO 10993-11:2007. Annex A.7,[52] test for systemic toxicity. Acute intraperitoneal application and a USP 41/NF 36:2018, systemic injection test was done using the OECD principles of GLP. Ten mice were used for the study (5 for the TiGNG1, and 5 for the Control samples). The body weight range of the animals was 17–23 g. Animals were maintained in a controlled environment with a temperature of 22 ± 3 °C, humidity of 30–70% and a light/dark cycle of 12 h. There was a minimum of 15 fresh air changes per hour. The 50 mL kg^{-1} cotton seed oil extract of the TiGNG1 and the control (cottonseed oil) were injected intraperitoneally into the mice and animals were observed immediately after injection and at 4, 24, 48, and 72 h for evidence of abnormalities like any clinical signs, loss of body weight or death.

1.18.2 Acute intraperitoneal application of saline extract of TiGNG1 in Swiss albino mice. A similar experiment was conducted using physiological saline extract of TiGNG1 according to the standard ISO 10993-11:2017, Annex A.8, test for systemic toxicity testing: acute intraperitoneal application[53] and a USP 41/NF 36:2018, systemic injection test following OECD principles of GLP. Ten mice were used for the study (5 for the TiGNG1, and 5 for the control samples). The body weight range of the animals was 17–23 g. Animals were maintained in a controlled environment with a temperature of 22 ± 3 °C, humidity of 30–70% and a light/dark cycle of 12 h. There was a minimum of 15 fresh air changes per hour. A 50 mL kg^{-1} saline extract of the TiGNG1 and the control (saline) was injected intraperitoneally into the mice and the animals were observed immediately after injection and at 4, 24, 48, and 72 h for the evidence of abnormalities like any clinical signs, loss of body weight or death.

1.19 Statistical analysis

One-way ANOVA followed by Tukey's test was used for statistical analysis between groups. All statistical analyses were performed using the software GraphPad Prism version 9.5.1.

2. Results

The copolymer of poly(acrylic acid-*co*-itaconic acid-*co*-*N*-vinyl pyrrolidone), poly(AA-*co*-IA-*co*-VP), was synthesized *via* free radical solution polymerization using ammonium persulfate as initiator and isopropyl alcohol as a chain transfer agent in an aqueous medium. The schematic representation for the synthesis of poly(AA-*co*-IA-*co*-VP) was shown in Fig. 1. The resulting polymer solution was rotary evaporated to remove unreacted monomers. Half a portion of the purified poly(AA-*co*-IA-*co*-VP) powder was dissolved in distilled water to prepare a 45% polyalkenoic acid solution and stored in an amber-coloured plastic bottle for GIC preparation. A thorough physicochemical

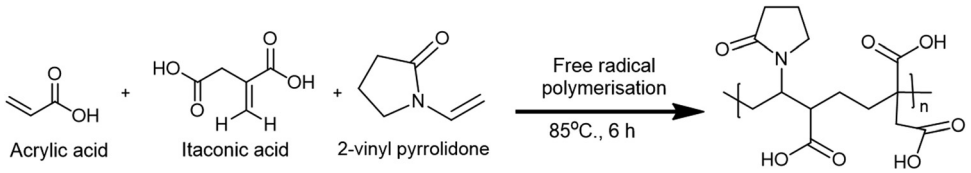

Fig. 1 Schematic representation for the synthesis of polyalkenoic acid [poly(AA-*co*-IA-*co*-VP)] using acrylic acid, itaconic acid and 2-vinyl pyrrolidone *via* a free radical solution polymerization technique.

characterization was performed using the other half of poly(AA-*co*-IA-*co*-VP).

The absence of monomer content in poly(AA-*co*-IA-*co*-VP) was confirmed using FTIR (Fig. 2A). A broad peak at 3421 cm^{-1} is associated with the –O–H stretching of the carboxylic group. The broadening of the peak was due to the inter or intra-molecular hydrogen bonding present in poly(AA-*co*-IA-*co*-VP). The strong absorption at 1699 cm^{-1} is associated with the –C═O stretching of the carboxylic acid. However, there is no ═C–H bending peak around 810 cm^{-1} in poly(AA-*co*-IA-*co*-VP), attributed to the complete consumption of the monomers. Nuclear magnetic resonance (NMR) spectra were analyzed to confirm the formation of poly(AA-*co*-IA-*co*-VP). The NMR analysis showed no acrylic peaks within 5.5–7 ppm, attributed to the absence of residual monomer content in the poly(AA-*co*-IA-*co*-VP). Here, the C–H group of *N*-vinyl pyrrolidone appeared at ~4.321 ppm. The peak at ~3.389 ppm showed the presence of itaconic acid in the copolymer. The –C–H group of acrylic acid showed a triplet at 3.909 ppm. The CH2 group near the nitrogen atom of the pyrrolidone ring showed a peak at 2.736 ppm (Fig. 2B).

The purity of poly(AA-*co*-IA-*co*-VP) was analyzed using HPLC residual monomer content (Fig. S1, ESI†). At first standard curves for all the monomers were prepared using different concentrations of acrylic acid, itaconic acid, and *N*-vinyl pyrrolidone. Based on the standard curves, residual monomer content was analyzed. HPLC data showed the presence of 0.9831 g acrylic acid, 0.3519 g itaconic acid, and 0.0178 g vinyl pyrrolidone per kilogram of poly(AA-*co*-IA-*co*-VP). It corresponds to 0.098 wt%, 0.035 wt%, and 0.0017 wt% acrylic acid, itaconic acid, and *N*-vinyl pyrrolidone, respectively. That means the residual monomer content detected was low and within the acceptable limit according to the standard. The molecular weight of poly(AA-*co*-IA-*co*-VP) was measured using gel permeation

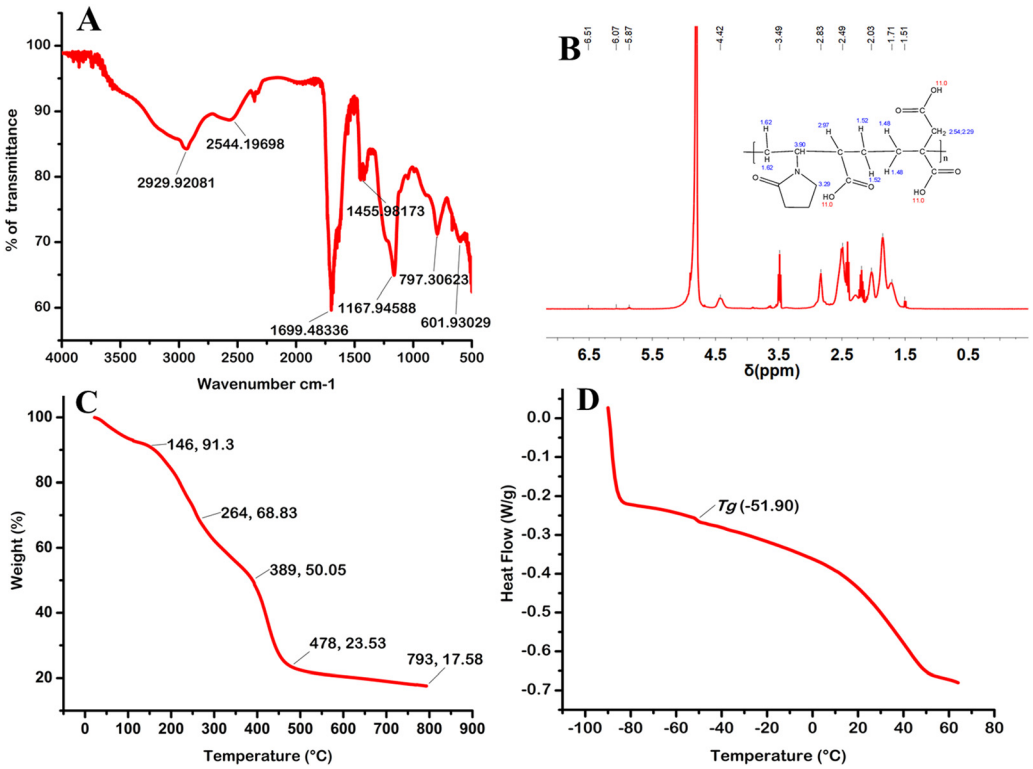

Fig. 2 (A) FTIR spectrum of poly(AA-*co*-IA-*co*-VP) showing complete consumption of the acrylic group, with no acrylic peak at ~810 cm^{-1}. (B) NMR spectrum of poly(AA-*co*-IA-*co*-VP) confirming the absence of residual acrylic groups, (C) thermogravimetric analysis showing the degradation profile of poly(AA-*co*-IA-*co*-VP), ~82% degradation within 800 °C, and (D) DSC curve displaying a glass transition temperature (T_g) of −51.90 °C for poly(AA-*co*-IA-*co*-VP).

chromatography (Fig. S2, ESI†). The data showed an average molecular weight (M_w) of 51.210 kDa, and a polydispersity index (PDI) of 1.26. Thermogravimetric analysis of polyalkenoic acid was obtained by plotting the % weight against temperature. The thermogram consists of 5 stages of decomposition. 8% of the sample gets degraded within 100 °C, which could be attributed to the residual water content in the sample. A gradual weight reduction was observed with an increase in temperature. At 265 °C, 31% of the material was degraded, followed by ~82% degradation at 800 °C. (Fig. 2C). DSC results indicated that poly(AA-*co*-IA-*co*-VP) has two glass transition temperatures (T_g) of 18.27 °C and 46.35 °C. This can be attributed to two types of blocks in the copolymer, poly(AA-*co*-IA-*co*-VP). (Fig. 2D).

Ionogels were prepared using a two-step reaction. First, ionic liquid was synthesized *via* an addition reaction of dibromobutane and 1-vinyl imidazole (Fig. 3). The structure of 3,3′-(butane-1,4-diyl)bis(1-vinyl-1*H*-imidazol-3-ium) bromide (DVIMBr) was confirmed using ^{1}H NMR (Fig. 5D). The spectra showed a sharp single peak observed at δ 1.9 ppm corresponding to the alkane chain –CH2 peaks. In addition, a peak appearing as a singlet at 4.2 ppm indicates the alkyl –CH2 peak adjacent to the nitrogen cation species. The peak at δ 9.1 ppm corresponds to the aromatic hydrogen peak within the imidazolium ring. The chemical shifts at 5.3 and 5.7 ppm correspond to the CH and CH2 peaks of vinyl groups, respectively, with one end connected to the nitrogen atom in the imidazolium ring. The FTIR spectra and thermal properties of both the monomer and the ionogel were evaluated (Fig. S3 and S4, ESI†). Then an ionic liquid-based nanogel called an ionogel was synthesized through free radical solution polymerization using DVIMBr and ethylene glycol dimethacrylate. To adjust the size of the ionogel, 20 mol% of mercaptoethanol was utilized as a chain transfer agent. The formation of the ionogel was confirmed by using FTIR and particle size measurements (Fig. 4A and B). The acrylic peak of EGDMA at 815 cm^{-1} disappeared after ionogel formation, as indicated by the absence of the =C–H bending peak at 815 cm^{-1} in the FTIR spectrum of the ionogel. The particle size distribution of the ionogel was analyzed after suspending the ionogel in DI water. The average particle size measured was 513 nm at a PDI of 0.183.

Fluoroaluminosilicate glass powder was synthesized *via* melting at a temperature of 1200 °C, followed by quenching in room temperature distilled water at a high yield of ~96%. SEM analysis showed non-uniform particles in the size range of 5 μm to 50 μm. An average particle size of 10 μm was dominated in the glass powder as shown in Fig. 5A and B. Glass ionomer cement (GIC) was prepared at different P/L ratios and characterized for their working time, setting time, compressive strength, diametrical tensile strength, and radiopacity. It was interesting to know that as the P/L ratio increased both the working time and setting time decreased. The Fig. 5C confirmed the presence of elements including aluminium (Al), silicon (Si), calcium (Ca), fluorine (F), and oxygen (O) in the glass powder. As visible in the spectra, the percentage of Al and Si was high.

Glass ionomer cements were prepared using an aqueous solution of 45% polyalkenoic acid formulation containing different weight percentages of ionogel (say 0.5 wt%, 1 wt%, 2 wt%) and the glass powder at a P/L ratio of 2.7. In addition to ionogel, L-tartaric acid was employed in a polyalkenoic acid formulation to manipulate the working and setting times of the GIC (Fig. 6A and B). Increasing the concentration of L-tartaric acid increased the working time of the GIC. Regardless of the available reports, 1% and 3% of MgO nanoparticles in 5% L-tartaric acid/polyalkenoic acid solution lead to a reduction in the working time of the GIC. The GICs prepared using 5% L-tartaric and 15% L-tartaric acid in the polyalkenoic acid formulation were labeled as TA-5 and TA-15. In contrast, GICs prepared using the above L-tartaric acid/polyalkenoic acid formulation and glass powder with additives 1% and 3% of MgO nanoparticles were represented as TA5M1, TA5M3, TA15M1, TA15M3 *etc.* The data showed that with a 5% L-tartaric acid-based polyalkenoic acid formulation, the working time decreased to ~48 s and ~39 s respectively for 1% and 3% of MgO nanoparticles. The 15% L-tartaric acid in the polyalkenoic acid formulation with 1 wt% and 3 wt% of MgO nanoparticles showed a working time of 67 s and 71 s, respectively. The results showed that L-tartaric acid had a substantial impact on increasing the working time of the GIC. However, MgO has no significant effect on improving the working time, contradictory

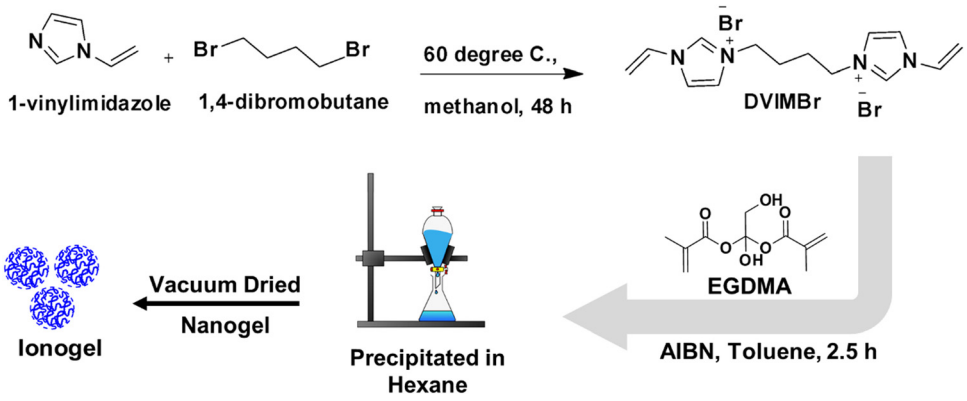

Fig. 3 Schematic representation of the synthesis of an ionogel *via* a two-step process.

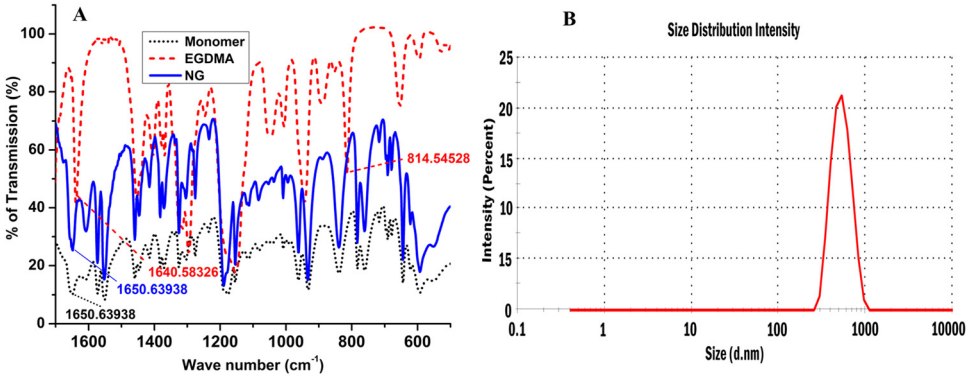

Fig. 4 (A) FTIR spectra of the ionogel (NG), EGDMA and DVIMBr (monomer). EGDMA showed an acrylic peak at ~815 cm^{-1}. The acrylic peak disappeared in the spectrum of the ionogel, indicating the complete consumption of EGDMA during ionogel synthesis. (B) Particle size distribution of the ionogel showing an average particle size of 513 nm.

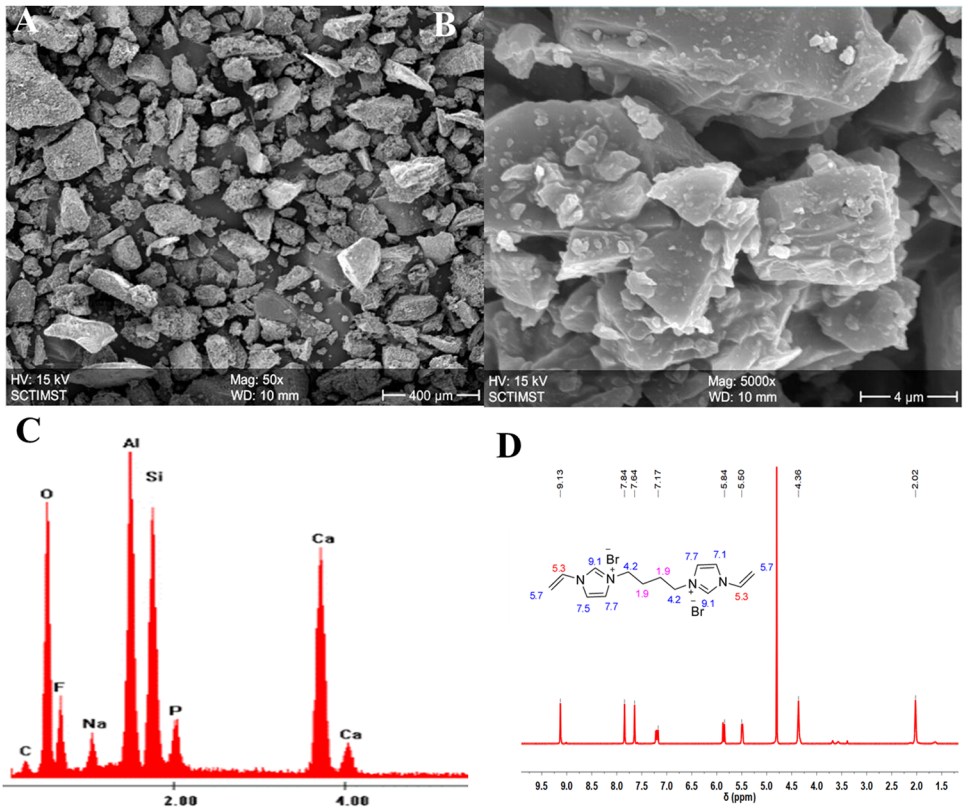

Fig. 5 (A) SEM image of the glass powder with magnification of (A) 50× and (B) 5000×. (C) EDAX spectra of the glass powder showed the presence of elements such as aluminum (Al), silicon (Si), calcium (Ca), oxygen (O), fluorine (F), *etc.* (D) NMR spectra of the ionic liquid (DVIMBr) showed acrylic peaks at ~5.3 ppm and 5.7 ppm.

to the existing report. The working time of the GIC prepared using 15% tartaric acid/polyalkenoic acid formulation with 1% ionogel was evaluated. The data showed a working time of 71 s and a setting time of 194.8 s for the ionogel-incorporated GIC.

Compressive strength of GIC at different weight% of ionogel additives, say 0 wt% NG; (GNG-0), 1 wt% NG; (GNG-1), 2 wt% NG; (GNG-2), and 5 wt% NG; (GNG-5%), were prepared and analyzed. GNG-0 showed a compressive strength of 38 MPa. As evident from Fig. 7A, the ionogel increased the compressive strength of the GIC. GNG-1 showed a compressive strength of 40.5 MPa. The compressive strength was not significantly different from GNG-0 (p-value = 0.6796). 2 wt% ionogel significantly improved the compressive strength of GNG-2 and showed an average compressive strength of 50.4 MPa with a p-value = 0.0005. GNG-5 showed an average compressive strength of 45.7 MPa. The compressive strength of GNG-5

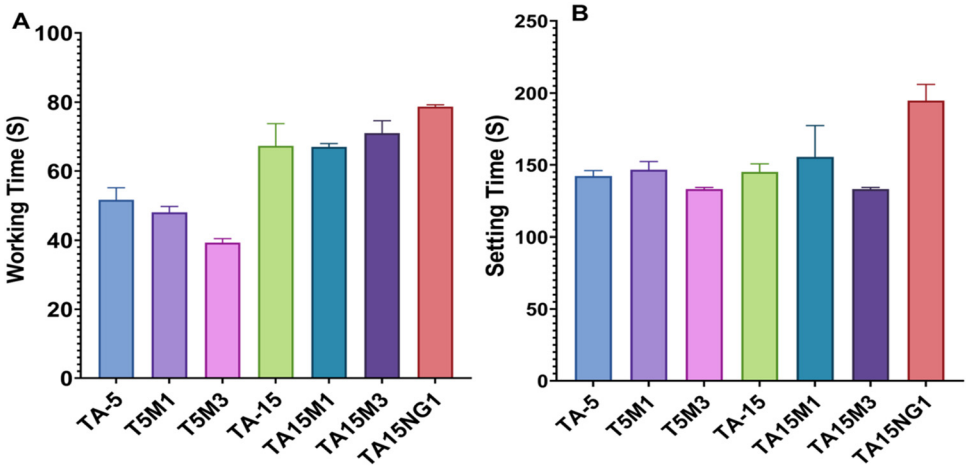

Fig. 6 (A) Working time of the glass ionomer cement with respect to different additives such as tartaric acid (TA-5 and TA-15) with 1% and 3% MgO nanoparticles (TA5M1, TA5M3, TA15M1 and TA15M3) and 1 wt% ionogel (TA15NG1). (B) Setting time of the glass ionomer cement with respect to different additives.

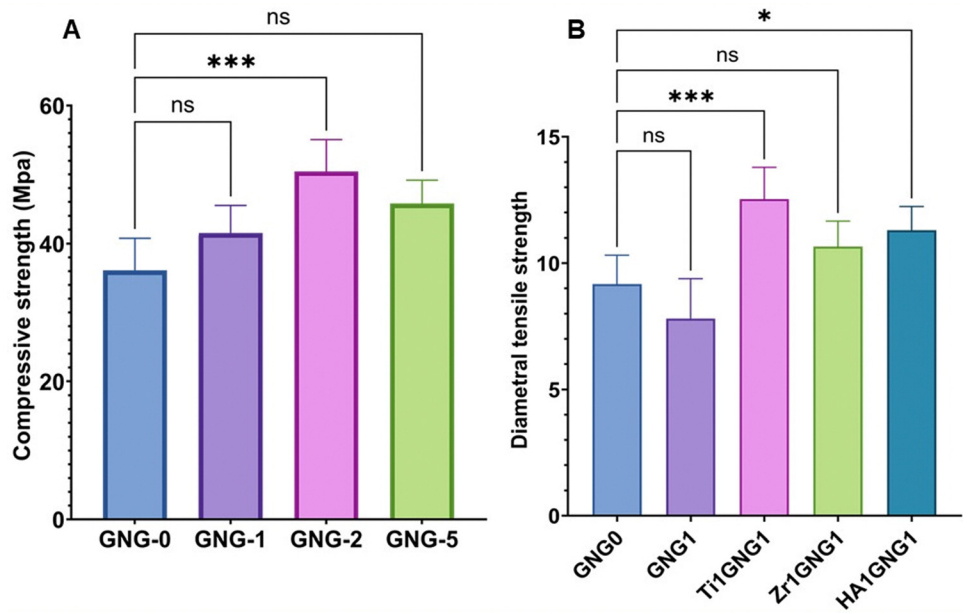

Fig. 7 (A) Compressive strength of ionogel modified glass ionomer cement (GNG) at different weight percentages of ionogel in the polyalkenoic acid formulation. (B) Diametrical tensile strength of the ionogel modified glass ionomer cement (GNG1) with 1 wt% TiOH (Ti1GNG1), HA (HA1GNG1), and ZrOH (Zr1GNG1).

reduced to 9.32% compared to GNG-2. Ionogel additives improved the compressive strength of GIC up to 2 wt%.

To enhance the mechanical properties of GIC, various additives have been used, including titanium oxide nanoparticles (TiOH), zirconium oxide microparticles (ZrOH), and hydroxyapatite nanoparticles (HA), as well as different weight percentages of ionogel. The weight ratio of traditional dental additives TiOH, HA, and ZrOH was set at 1 wt% (Fig. 8A and B). As indicated in the picture, GICs containing 0.5 wt% ionogel and 1 wt% additives such as TiOH, Zr–OH, and HA had compressive strengths of 50.67 MPa (p = 0.070), 37.30 MPa (p = 0.999), and 39.59 MPa (p = 0.999), respectively. Incorporating 1 wt% of TiOH, Zr–OH, and HA to GNG 1 resulted in compressive strengths of 128.70 MPa ($p < 0.0001$), 111.77 MPa ($p < 0.001$), and 90.27 MPa ($p < 0.001$), respectively. Ionogels had a substantial influence on the compressive strength of GIC. Furthermore, conventional dental additives in GNG2 showed a compressive strength of 59.90 MPa ($p = <0.0001$), 49.85 MPa ($p = <0.0133$), and 58.34 MPa ($p = <0.0001$) respectively. A drastic reduction in the compressive strength of GNG 2 was observed in the presence of TiOH, HA, and ZrOH.

This study optimized the effect of ionogel with various additives such as TiOH, ZrOH and HA to improve the mechanical properties of GIC. GNG2 showed a significant improvement in compressive strength compared to GNG0 where no ionogel additives were involved. However, adding conventional additives to the GNG2 formulation reduced the compressive strength drastically. In contrast, GNG1 showed improved

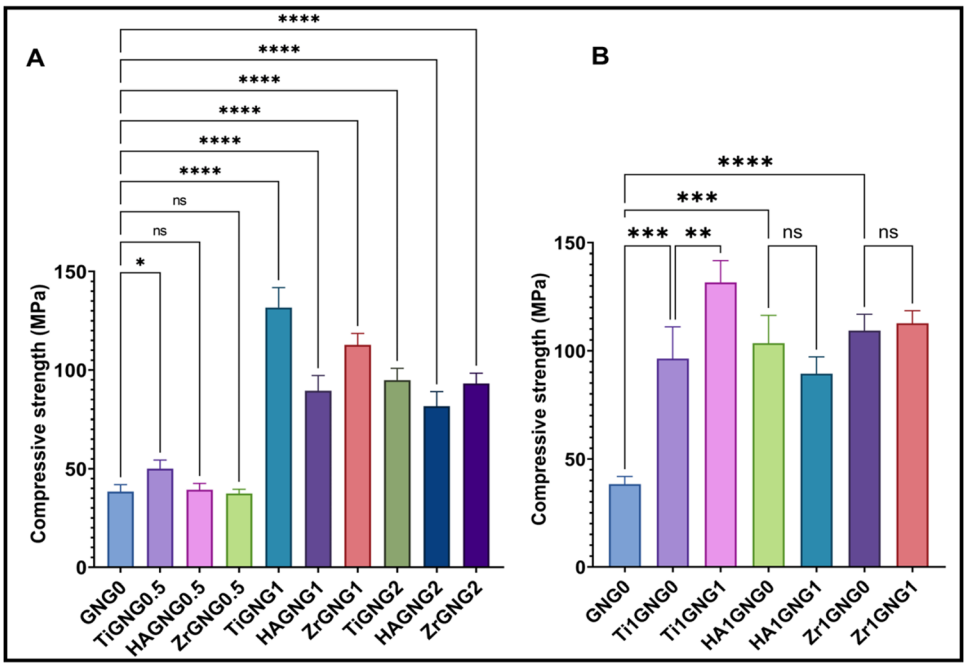

Fig. 8 (A) Compressive strength of glass ionomer cement with ionogel additives (0.5 wt%, 1 wt% and 2 wt%) in the presence of 1 wt% TiOH, HA, and ZrOH. (B) A comparison graph for the compressive strength of glass ionomer cement with ionogel additives (0 wt%, 1 wt%) in the presence of 1 wt% TiOH (Ti1GNG1), HA (HA1GNG1), and ZrOH (Zr1GNG1).

compressive strength (Fig. 8). The other dental additives in the glass powder were limited to 1 wt% as several previous studies proved that more additives in glass reduce its mechanical properties. GIC with bare glass powder showed a compressive strength of 37 MPa only. The compression strength of 1 wt% of TiOH in GIC showed an increase of 172% compared to GNG0. On the other hand, 1 wt% of ZrOH and HA in GNG1 showed a compressive strength enhancement of 175% and 197%, respectively compared to the GNG0.

The diametrical tensile strength (DTS) of glass ionomer cement with 1 wt% ionogel (GNG1) in combination with 1 wt% TiOH, or 1 wt% HA or 1 wt% ZrOH is shown in Fig. 7B. The glass ionomer cement without ionogel (GNG0) was used as a control. The GNG-0 showed a DTS value of 4.77 MPa. The addition of 1 wt% ionogel showed a DTS value of 6.85 MPa. Furthermore, the incorporation of 1 wt% TiOH to the GNG1 resulted in the highest DTS value of 12.03 MPa. Similarly, 1 wt% ZrOH and 1 wt% HA added to GNG1, ZrGNG1 and HAGNG1 respectively, showed a DTS value of 10.53 MPa and 11.16 MPa. This result highlighted the importance of using ionogel with TiOH/HA/ZrOH additives in the conventional GIC to improve the mechanical properties.

Radiopacity is an important factor when considering dental restorative materials. The radiopaque dental materials enable the clinician to radiographically diagnose secondary caries and marginal defects which are usually located on the proximal gingival margin. The radiopacity of GIC prepared at a P/L ratio of 2.7 was evaluated using micro-CT. Four different GIC samples were analyzed; C-glass (GIC prepared using commercially available glass powder and polyalkenoic acid optimized in the lab), GNG1 (1 wt% ionogel modified glass ionomer cement), CGIC-1 (commercially available GIC having less radiopacity), and CGIC-2 (commercially available GIC having high radiopacity). As evident from Fig. 9B, polyakenoic acid formulations optimized in the laboratory didn't show any radiopaque characteristics. Two commercial GICs were used as predicate device controls in which CGIC-2 was highly radiopaque and CGIC-1 was less radiopaque. The white colour indicates radiopacity and the grey colour indicates no/low radiopacity. GNG1 showed

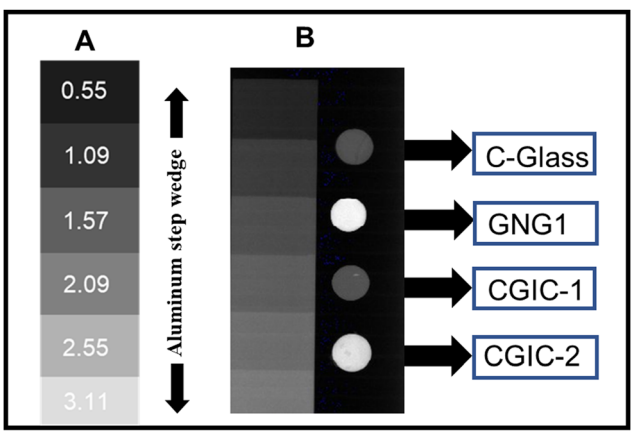

Fig. 9 (A) Different thickness (mm) of aluminum step wedge. (B) Radiopacity of the aluminum step wedge, C-glass (GIC prepared using commercial glass and in-house polymer), GNG1 (in-house GIC with 1% ionogel), and CGIC-1 and CGIC-2 as different commercial GIC samples as controls.

high radiopacity and was comparable to the commercially available radiopaque formulation and appeared white.

2.1 *In vitro* cytotoxicity

In vitro cytotoxicity studies were conducted based on the standard, ISO 10993-5. The conventional glass ionomer cement and titanium oxide nanoparticle modified ionogel impregnated glass ionomer cement (TiGNG1) showed no significant morphological changes for L929 mouse fibroblast cells during the treatment. The negative control, GNG0 and TiGNG1 showed no detectable zone of lysis, vacuolization or detachment and thereby confirmed the none cytotoxic reactivity (Fig. 10). However, the positive control gave severe cytotoxic reactivity as expected.

2.2 *In vivo* evaluation

2.2.1 Acute intraperitoneal application of cottonseed oil in Swiss albino mice. The schematic representation (Fig. 11) revealed different steps implemented for the biocompatibility evaluation of TiGNG1 using cotton seed extract and physiological saline extract of TiGNG1. The results indicated that the cotton seed oil extract of TiGNG1 and the control material did not show any abnormalities or significant loss in body weight during the observation period (Fig. 12B), thereby confirming their biocompatibility. Common clinical signs and observations are reported in Table T3 (ESI†). The cotton seed extract of TiGNG1 meets the biocompatibility requirement as per ISO 10993-11:2017(E), Annex A.7 Test for systemic toxicity: acute intraperitoneal application.

2.2.2 Acute intravenous application of physiological saline extract in Swiss albino mice. The results indicated that the physiological saline extract of TiGNG1 and the control (saline only) injected in the animals did not show any abnormalities or loss in body weight during the observation period (Fig. 12A). These results confirmed that the physiological saline extract of the TiGNG1 was nontoxic under the laboratory conditions simulated. Common clinical signs and observations are reported in Table T2 (ESI†). The physiological saline extract of TiGNG1 meets the requirement of the test as per ISO 10993-11:2017(E), Annex A.8 test for systemic toxicity: acute intravenous applications.

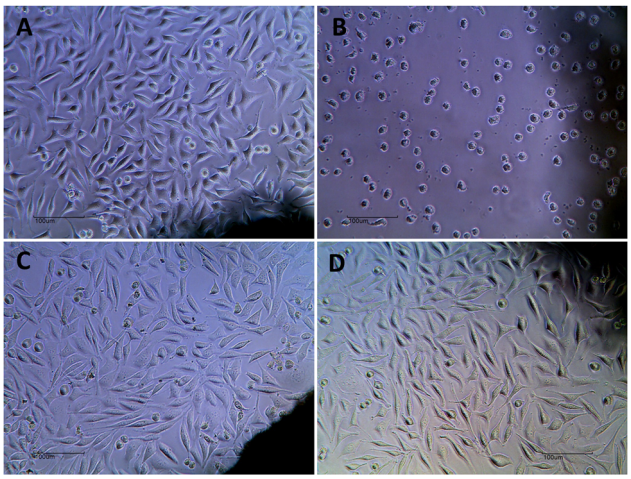

Fig. 10 L929 mouse fibroblast cells after 24 h direct contact with (A) negative control (ultrahigh molecular weight polyethylene, UHMWPE), (B) positive control (stabilized polyvinyl chloride, PVC disc), (C) glass ionomer cement without ionogel (GNG0) and (D) glass ionomer cement with 1 wt% ionogel and 1 wt% TiOH (TiGNG1); no change in the spindle morphology of L929 mouse fibroblast cells was observed after 24 h incubation with negative control, GNG0 and TiGNG1, indicating their cytocompatibility. On the other hand, the positive control treated cells lost their spindle morphology indicating its severe cytotoxic nature.

3. Discussion

This study focused on improving the mechanical properties of conventional glass ionomer cements using ionogel additives. Ionic liquid-based nanogels called ionogel additives improved the mechanical properties of GIC, as evidenced by the improved compressive strength. This may be attributed to the reduced intermolecular hydrogen bonding between poly(AA-*co*-IA-*co*-VP) polymer chains due to the strong interactions between ionogels and poly(AA-*co*-IA-*co*-VP). The interaction of the ionogel improved the availability of reactive functional groups in poly(AA-*co*-IA-*co*-VP) to bond with glass powder during the curing process. In addition to that, the zwitterionic nature of the ionic liquid could introduce antimicrobial properties to the base composition. However, the work was not focused on the antimicrobial characteristics of ionic liquids. The improved mixing compatibility was attributed to the zwitterionic nature of the ionic liquid, which provides multiple ionic functionalities to improve bonding within the cement network. The particle size and particle size distribution of the glass powder are key factors in modulating the mixing compatibility and working time of the GIC. In this study, glass powder with different particle sizes was observed in the SEM image. The smaller glass particles increased the surface area of the glass powder, and the larger particles improved the mechanical strength of the GIC. The synergistic effect of different particle sizes of glass powder improved the physicochemical characteristics of the GIC.

As evident from the literature, the working time and setting time of GIC can also be altered by the strategic use of additives like L-tartaric acid and MgO nanoparticles.[53–55] The current study also demonstrated the positive effect of L-tartaric acid in delaying the working time of the GIC. Initially, the incorporation of 5 wt% tartaric acids into polyalkenoic acid resulted in a working time of 51 s. The increased concentration of tartaric acid led to an extension of the setting time of the GIC and the incorporation of 15 wt% tartaric acid into the polyalkenoic acid formulation, expanding the working time to 67 s. However, no significant effect was seen with MgO nanoparticles in modulating the working time and setting time of the GIC. This may be attributed to the difference in the composition of the optimized formulation of glass powder and polyalkenoic acid solution in the study compared to the reported literature. The interaction between ions in the glass powder, additives, and polyalkenoic acid formulation could strongly influence the working time and

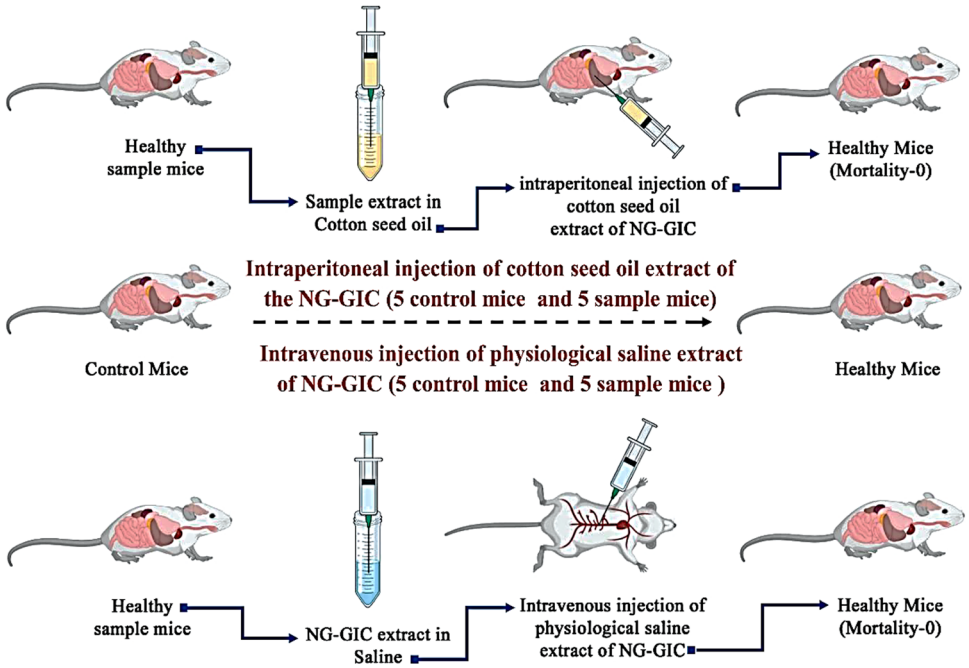

Fig. 11 Schematic representation of biocompatibility evaluation of TiGNG1 using cotton seed oil extract and physiological saline extract of TiGNG1.

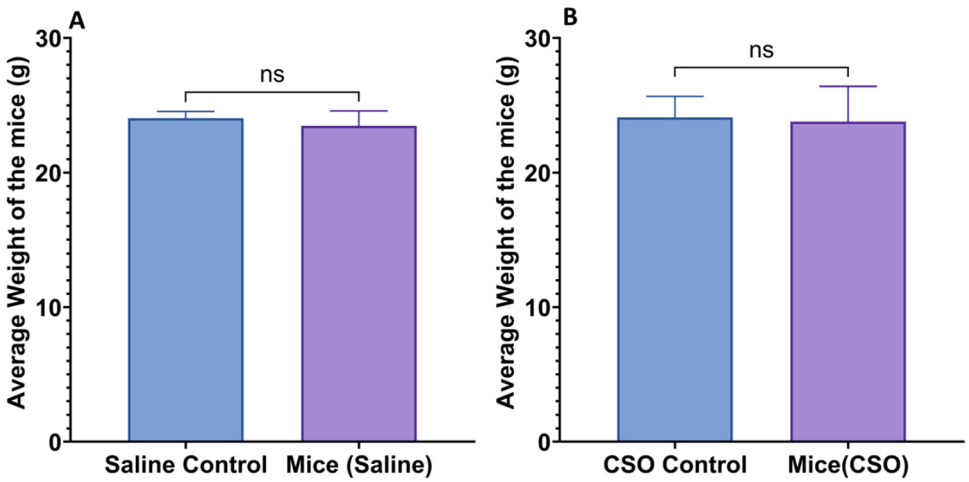

Fig. 12 Average weight of mice treated with (A) physiological saline extract of TiGNG1 (B) cotton seed oil (CSO) extract of TiGNG1.

mechanical properties of the GIC. The increasing working time with higher tartaric acid content could be attributed to its ability to control the acid–base setting reaction. The stereochemistry of the tartaric acid also plays a significant role in extending the working time. As reported earlier, both a racemic mixture and stereoisomers can alter the working time and setting time of GIC. However, the current formulation showed significant improvement with L-tartaric acid only. Based on the results, 15% L-tartaric acid-containing formulations were selected to investigate the effects of ionogel concentration in GIC.

The effects of ionogel in the GIC matrix have yielded significant insight into the alteration of its compressive strength. Here, GNG0, without any additives, showed a low compressive strength. The ionogel additives improved the compressive strength and established an optimum ionogel concentration of 2 wt% in the GIC formulation. Ionogel additive interfered with the intra- and intermolecular hydrogen bonding within the polyalkenoic acid solution. This hydrogen bonding interaction within the polyalkenoic acid formulation limits the availability of carboxylic acid groups that can react with ions in the glass powder and alter the setting reaction and the mechanical properties of the GIC.

Based on the literature, the study consistently maintained 1% of additives in the glass powder. A strong interaction of ionogel within the cement matrix happened in different ways, including ionic interaction and van der Waals force of interactions. The zwitterionic nature of the ionogel positively affected

interacting polyalkenoic acid formulations with multiple ions in the glass powder. The study indicated that the use of excess additives in GIC could lead to adverse effects on its mechanical properties. The overloading of additives hinders the ionic interaction between the glass powder and polyalkenoic acid formulation.

This study demonstrated that incorporating one wt% ionogel and 1 wt% TiOH nanoparticle in the formulation enhanced its compressive strength to 128.70 MPa. The mechanical properties of the modified GIC could be suited for clinical application according to ISO 9917-1 standard, which specifies that compressive strength of more than 100 MPa will be eligible for glass polyalkenoate. 1 wt% ionogel-modified glass ionomer cement with one wt% TiOH additive (TiGNG-1) was finalized for further biocompatibility evaluations. Both *in vitro* and *in vivo* studies were performed using TiGNG1. *In vitro* cytotoxicity studies revealed the non-cytotoxic effects of TiGNG1. The addition of ionogel did not introduce any toxicity. Animal studies were performed using Swiss albino rats using the extract of TiGNG1. Both cotton seed oil extract and saline extract of TiGN1 were studied. An acute intraperitoneal application of cotton seed oil extract of GNG-1 in Swiss albino mice reveals that TiGNG1 extract and control CSO-injected mice exhibited normal behavior and consistently maintained body weights throughout the observation period and were non-disruptive to the animal's well-being.

Similarly, intravenous application of a physiological saline extract of TiGNG1 also does not lead to any abnormalities or loss of body weight throughout the testing time. The saline and cotton seed oil extract (CSO) of TiGNG1 showed no toxic effects under the simulated lab conditions. During the experiment, a few criteria were prefixed, such as the occurrence of two or more deaths among the mice, abnormal behaviors such as convulsions or prostration in two or more mice, or a body weight loss exceeding 2 g in three or more mice included for the criteria for potential toxicity. The results demonstrated no adverse effect of TiGNG1 in any experimental mice, confirming the biocompatibility of the ionogel-modified glass ionomer cement.

4. Limitations of the study

The study focused on the mechanical property improvement of glass ionomer cement (GIC) using ionogel additives. Even though the mechanical properties of GIC improved with the addition of 2 wt% ionogel (*i.e.*, 32.6% improvement in the compressive strength), the improvement is not sufficient based on the ISO 9917-1 standard. However, the addition of 1 wt% titanium oxide nanoparticle (TiOH), zirconium oxide microparticles (ZrOH), and hydroxyapatite nanoparticles (HA) along with ionogel additives showed a compressive strength of 128.70 MPa, 111.77 MPa, and 90.27 MPa, respectively.

Author contributions

MS contributed to the conceptualization and design of the study. MS won funding for the study. MS and SL contributed to the acquisition of laboratory data and data curation. MS and SL performed formal data analysis and contributed to the formal interpretation of the data. SL and MS wrote the original draft. MS critically revised the manuscript. MS was involved in editing and approving the final version of the manuscript.

Future scope

Antimicrobial activities of ionogel-impregnated glass ionomer cement need to be established.

Disclosure

All animal experiments were performed in compliance with the Institutional Animal Ethics Committee (No. SCT/IAEC-346/May/2020/105). The study was conducted as per the requirements of the ISO 10993-11:2007. Annex A.7 and Annex A.8, test for systemic toxicity: acute systemic toxicity test: acute intraperitoneal application and the USP41/NF 36:2018, systemic injection test (study no. WITOXQ71.23) was done using OECD principles of GLP.

Data availability

All raw data will be available on request.

Conflicts of interest

There are no conflicts to declare.

Acknowledgements

The authors gratefully acknowledge the start-up research grant (SRG/2020/001600), Science and Engineering Research Board (SERB), Department of Science and Technology, Govt. of India for funding. The authors would like to thank the Director, SCTIMST and the Head, of the BMT wing, SCTIMST for the facilities provided to carry out this work. The authors greatly acknowledge the efforts of Dr Deepu D. R. for mechanical testing.

References

1 R. Bharti, K. K. Wadhwani, A. P. Tikku and A. Chandra, Dental amalgam: an update, *J. Conservative Dent.*, 2010, **13**(4), 204–208, DOI: **10.4103/0972-0707.73380**.
2 H. H. Hamama, Recent advances in posterior resin composite restorations, *Appl. Nanocompos. Mater. Dent.*, 2019, 319–336, DOI: **10.1016/B978-0-12-813742-0.00019-5**.
3 T. De Caluwé, C. W. J. Vercruysse, S. Fraeyman and R. M. H. Verbeeck, The influence of particle size and fluorine content of aluminosilicate glass on the glass ionomer cement properties, *Dent. Mater.*, 2014, **30**, 1029–1038, DOI: **10.1016/J.DENTAL.2014.06.003**.

4 I. Denry and J. A. Holloway, Ceramics for Dental Applications: A Review, *Materials*, 2010, **3**, 351–368, DOI: **10.3390/ma3010351**.
5 J. W. Nicholson, Chemistry of glass-ionomer cements: a review, *Biomaterials*, 1998, **19**, 485–494, DOI: **10.1016/S0142-9612(97)00128-2**.
6 S. K. Sidhu and J. W. Nicholson, A Review of Glass-Ionomer Cements for Clinical Dentistry, *J. Funct. Biomater.*, 2016, **7**(16), DOI: **10.3390/jfb7030016**.
7 M. S. Baig and G. J. P. Fleming, Conventional glass-ionomer materials: a review of the developments in glass powder, polyacid liquid and the strategies of reinforcement, *J. Dent.*, 2015, **43**, 897–912, DOI: **10.1016/J.JDENT.2015.04.004**.
8 I. M. Bezerra, A. C. M. Brito, S. A. de Sousa, B. M. Santiago, Y. W. Cavalcanti, L. de and F. D. de Almeida, Glass ionomer cements compared with composite resin in restoration of noncarious cervical lesions: a systematic review and meta-analysis, *Heliyon*, 2020, **6**, e03969, DOI: **10.1016/j.heliyon.2020.e03969**.
9 L. A. Dobrzá Nski, L. B. Dobrzá Nski, A. D. Dobrzá Nska-Danikiewicz and J. Dobrzá Nska, The Concept of Sustainable Development of Modern Dentistry, *Processes*, 2020, **8**, 1605, DOI: **10.3390/pr8121605**.
10 B. E. Kent, B. G. Lewis and A. D. Wilson, Glass Ionomer Cement Formulations, *J. Dent. Res.*, 1979, **58**, 1607–1619, DOI: **10.1177/00220345790580061001**.
11 J. F. McCabe, Resin-modified glass-ionomers, *Biomaterials*, 1998, **19**, 521–527, DOI: **10.1016/S0142-9612(98)00132-X**.
12 L. C. Pereira, M. C. P. Nunes, R. G. P. Dibb, J. M. Powers, J.-F. Roulet, M. F. de and L. Navarro, Mechanical properties and bond strength of glass-ionomer cements, *J. Adhes. Dent.*, 2002, **4**, 73–80.
13 D. Xie, W. A. Brantley, B. M. Culbertson and G. Wang, Mechanical properties and microstructures of glass-ionomer cements, *Dent. Mater.*, 2000, **16**, 129–138, DOI: **10.1016/S0109-5641(99)00093-7**.
14 M. S. de Moura, G. P. de Sousa, M. H. S. F. Brito, M. C. C. Silva, M. D. D. M. de Lima, L. de Fátima Almeida de Deus Moura, R. C. Pascotto and C. C. B. Lima, Does low-cost GIC have the same survival rate as high-viscosity GIC in atraumatic restorative treatments? A RCT, *Brazil Oral. Res.*, 2019, **33**, 1–11, DOI: **10.1590/1807-3107BOR-2019.VOL33.0125**.
15 A. D. Wilson and B. G. Lewis, The flow properties of dental cements, *J. Biomed. Mater. Res.*, 1980, **14**(4), 383–391, DOI: **10.1002/jbm.820140405**.
16 A. J. Noori and F. A. Kareem, Setting time, mechanical and adhesive properties of magnesium oxide nanoparticles modified glass-ionomer cement, *J. Mater. Res. Technol.*, 2020, **9**, 1809–1818, DOI: **10.1016/J.JMRT.2019.12.012**.
17 D. M. Kyrios, E. S. Duke and A. S. Windeler, Glass-ionomer cement film thickness and working time, *J. Prosthet. Dent.*, 1989, **62**, 533–536, DOI: **10.1016/0022-3913(89)90074-7**.
18 N. Panahandeh, E. Hasani, S. Safa, M. Hashemi and H. Torabzadeh, Effects of Incorporation of Titanium Dioxide Nanoparticles on Mechanical Properties of Conventional Glass Ionomer Cement, *J. Iran. Med. Council*, 2023, **7**, 99–106, DOI: **10.18502/jimc.v7i1.14206**.
19 K. R. Kantovitz, F. P. Fernandes, I. V. Feitosa, M. O. Lazzarini, G. C. Denucci, O. P. Gomes, P. A. Giovani, K. M. S. Moreira, V. G. A. Pecorari, A. F. S. Borges, F. H. Nociti, R. T. Basting, P. N. Lisboa-Filho and R. M. Puppin-Rontani, TiO_2 nanotubes improve physico-mechanical properties of glass ionomer cement, *Dent. Mater.*, 2020, **36**, e85–e92, DOI: **10.1016/J.DENTAL.2020.01.018**.
20 V. P. Pranav, P. Vanajassun, M. S. Nivedhitha, N. T. Nishad and D. Soman, Effects of Zinc Oxide Nanoparticles in Combination with Conventional Glass Ionomer Cement: *In vitro* Study, *Adv. Hum. Biol.*, 2014, **4**, 31–36.
21 D. AlMatar, S. AlSanousi, J. Ahmed and S. Saad Bin Qasim, The *In Vitro* Effect of Silver and Zinc Oxide Nanoparticles on Fluoride Release and Microhardness of a Resin-Modified Glass Ionomer Cement, *J. Inorg. Organomet. Polym. Mater.*, 2023, **33**, 1507–1516, DOI: **10.1007/s10904-023-02551-w**.
22 M. Bilić, B.-P. Prcić, V. Brzovićbrzović, R. Rajić, A. Ivanišević ivanišević, A. Pilipovićpilipović, S. Gurgan and I. M. Miletić, Mechanical Properties of Glass Ionomer Cements after Incorporation of Marine Derived Hydroxyapatite, *Materials*, 2020, **13**, 3542, DOI: **10.3390/ma13163542**.
23 R. A. S. Alatawi, N. H. Elsayed and W. S. Mohamed, Influence of hydroxyapatite nanoparticles on the properties of glass ionomer cement, *J. Mater. Res. Technol.*, 2019, **8**, 344–349, DOI: **10.1016/J.JMRT.2018.01.010**.
24 W. Nurshamimi, W. Jusoh, K. Amin Matori, M. Hafiz, M. Zaid, N. Zainuddin, M. Zulhasif, A. Khiri, N. Asyikin, A. Rahman, R. A. Jalil, E. Kul, W. N. Matori, K. A. Mohd, M. H. Zaid, N. Zainuddin, A. Jalil and R. Kul, Incorporation of Hydroxyapatite into Glass Ionomer Cement (GIC) Formulated Based on Alumino-Silicate-Fluoride Glass Ceramics from Waste Materials, *Materials*, 2021, **14**, 954, DOI: **10.3390/ma14040954**.
25 A. Prabhakar, P. Kalimireddy, C. Yavagal and S. Sugandhan, Assessment of the clinical performance of zirconia infused glass ionomer cement: an *in vivo* study, *Int. J. Oral Health Sci.*, 2015, **5**, 74, DOI: **10.4103/2231-6027.178501**.
26 Y. W. Gu, A. U. J. Yap, P. Cheang and K. A. Khor, Zirconia–glass ionomer cement––a potential substitute for Miracle Mix, *Scr. Mater.*, 2005, **52**, 113–116, DOI: **10.1016/J.SCRIPTAMAT.2004.09.019**.
27 A. A. Khan, A. Bari, A. Abdullah Al-Kheraif, H. Alsunbul, H. Alhaidry, R. Alharthi and A. Aldegheishem, Oxidized natural biopolymer for enhanced surface, physical and mechanical properties of glass ionomer luting cement, *Polymers*, 2023, **15**(12), 2679.
28 L. Paiva, T. K. S. Fidalgo, L. P. da Costa, L. C. Maia, L. Balan, K. Anselme, L. Ploux and R. M. S. M. Thiré, Antibacterial properties and compressive strength of new one-step preparation silver nanoparticles in glass ionomer cements (NanoAg-GIC), *J. Dent.*, 2018, **69**, 102–109, DOI: **10.1016/J.JDENT.2017.12.003**.
29 E. A. Altuntas, B. Özkan, S. Güngör and Y. Özsoy, Biopolymer-Based Nanogel Approach in Drug Delivery: Basic

Concept and Current Developments, *Pharmaceutics*, 2023, **15**, 1644, DOI: **10.3390/pharmaceutics15061644**.

30 A. Moshaverinia, S. Ansari, M. Moshaverinia, N. Roohpour, J. A. Darr and I. Rehman, Effects of incorporation of hydroxyapatite and fluoroapatite nanobioceramics into conventional glass ionomer cements (GIC), *Acta Biomater.*, 2008, **4**, 432–440, DOI: **10.1016/j.actbio.2007.07.011**.

31 J. Makanjuola and S. Deb, Chemically Activated Glass-Ionomer Cements as Bioactive Materials in Dentistry: A Review, *Prosthesis*, 2023, **5**, 327–345, DOI: **10.3390/prosthesis5010024**.

32 D. Xie, I. D. Chung, W. Wu and J. Mays, Synthesis and evaluation of HEMA-free glass–ionomer cements for dental applications, *Dent. Mater.*, 2004, **20**, 470–478, DOI: **10.1016/J.DENTAL.2003.07.003**.

33 M. M. Ahmed, M. S. M. Ameen, M. Abazari, S. M. Badeleh, K. Rostamizadeh and S. S. Mohammed, Chitosan-decorated and tripolyphosphate-crosslinked pH-sensitive niosomal nanogels for Controlled release of fluoropyrimidine 5-fluorouracil, *Biomed. Pharmacother.*, 2023, **164**, 114943, DOI: **10.1016/J.BIOPHA.2023.114943**.

34 Y. Bin Hamzah, S. Hashim and W. A. W. A. Rahman, Synthesis of polymeric nano/microgels: a review, *J. Polym. Res.*, 2017, **24**, 134, DOI: **10.1007/s10965-017-1281-9**.

35 B. M. Fronza, I. Y. Rad, P. K. Shah, M. D. Barros, M. Giannini and J. W. Stansbury, Nanogel-Based Filler-Matrix Interphase for Polymerization Stress Reduction, *J. Dent. Res.*, 2019, **98**, 779–785, DOI: **10.1177/0022034519845843**.

36 R. R. Moraes, J. W. Garcia, M. D. Barros, S. H. Lewis, C. S. Pfeifer, J. Liu and J. W. Stansbury, Control of polymerization shrinkage and stress in nanogel-modified monomer and composite materials, *Dent. Mater.*, 2011, **27**, 509–519, DOI: **10.1016/J.DENTAL.2011.01.006**.

37 E. G. Albeshir, R. Alsahafi, R. Albluwi, A. A. Balhaddad, H. Mitwalli, T. W. Oates, G. D. Hack, J. Sun, M. D. Weir and H. H. K. Xu, Low-Shrinkage Resin Matrices in Restorative Dentistry-Narrative Review, *Materials*, 2022, **15**, 1–21, DOI: **10.3390/ma15082951**.

38 A. V. Susila, Role of Composition on Polymerization Shrinkage and Shrinkage Stress in Dental Composites, *J. Operative Dent. Endod.*, 2021, **6**, 32–44, DOI: **10.5005/jp-journals-10047-0106**.

39 C. T. W. Meereis, E. A. Münchow, W. L. de Oliveira da Rosa, A. F. da Silva and E. Piva, Polymerization shrinkage stress of resin-based dental materials: a systematic review and *meta*-analyses of composition strategies, *J. Mech. Behav. Biomed. Mater.*, 2018, **82**, 268–281, DOI: **10.1016/J.JMBBM.2018.03.019**.

40 M. Suhail, J. M. Rosenholm, M. U. Minhas, S. F. Badshah, A. Naeem, K. U. Khan and M. Fahad, Nanogels as drug-delivery systems: a comprehensive overview, *Ther. Delivery*, 2019, **10**, 697–717, DOI: **10.4155/tde-2019-0010**.

41 F. Pinelli, Ó. F. Ortolà, P. Makvandi, G. Perale and F. Rossi, *In vivo* drug delivery applications of nanogels: a review, *Nanomedicine*, 2020, **15**, 2707–2727, DOI: **10.2217/nnm-2020-0274**.

42 S. V. Vinogradov, Nanogels in the race for drug delivery, *Nanomedicine*, 2010, **5**, 165–168, DOI: **10.2217/nnm.09.103**.

43 A. Moshaverinia, S. Ansari, Z. Movasaghi, R. W. Billington, J. A. Darr and I. U. Rehman, Modification of conventional glass-ionomer cements with *N*-vinylpyrrolidone containing polyacids, nano-hydroxy and fluoroapatite to improve mechanical properties, *Dent. Mater.*, 2008, **24**, 1381–1390, DOI: **10.1016/J.DENTAL.2008.03.008**.

44 M. Taghavikish, S. Subianto, N. K. Dutta and N. R. Choudhury, Facile Fabrication of Polymerizable Ionic Liquid Based-Gel Beads via Thiol–ene Chemistry, *ACS Appl. Mater. Interfaces*, 2015, **7**, 17298–17306, DOI: **10.1021/acsami.5b04405**.

45 C. Miao, F. Li, Y. Zuo, R. Wang and Y. Xiong, Novel redox-responsive nanogel based on poly(ionic liquid)s for the triggered loading and release of cargos, AIChE Annual Meeting, Conference Proceedings 2019-November (2016), DOI: **10.1039/C5RA21820A**.

46 J. Zhang, J. Liu, Y. Zuo, R. Wang and Y. Xiong, Preparation of Thermo-Responsive Poly(ionic liquid)s-Based Nanogels via One-Step Cross-Linking Copolymerization, *Molecules*, 2015, **20**, 17378–17392, DOI: **10.3390/molecules200917378**.

47 E. Bresciani, T. De, J. E. Barata, T. C. Fagundes, A. Adachi, M. M. Terrin, M. Fidela and L. Navarro, Compressive and Diametral Tensile Strength of Glass Ionomer Cements Resistência À Compressão E À Tração Diametral De Cimentos De Ionômero De Vidro, 2004. **https://www.fob.usp.br**.

48 D. Dalal, Comparitive Evaluation of Compressive Strength and Diametral Tensile Strength of Zirconomer, Ketac Molar And Type Ix Gic, 2018. **https://www.journalcra.com**.

49 P. P. Lizymol, Studies on Shrinkage, Depth of Cure, and Cytotoxic Behavior of Novel Organically Modified Ceramic Based Dental Restorative Resins, *J. Appl. Polym. Sci.*, 2010, **116**, 2645–2650, DOI: **10.1002/app.31762**.

50 ISO 10993-5 Biological evaluation of medical devices-Part 5: tests for *in vitro* cytotoxicity, 2009.

51 ISO 10993-11 Biological evaluation of medical devices-Part 11: tests for systemic toxicity 2017, International Organization for Standardization, Geneva, 2017.

52 ISO 10993-11:2007, Biological evaluation of medical devices—Part 11: tests for systemic toxicity, International Organization for Standardization, Geneva, 2007, Annex A.7.

53 F. Amin, S. Rahman, Z. Khurshid, M. S. Zafar, F. Sefat and N. Kumar, Effect of nanostructures on the properties of glass ionomer dental restoratives/cements: a comprehensive narrative review, *Materials*, 2021, **14**, 6260, DOI: **10.3390/ma14216260**.

54 H. Almira, E. Herda and Sunarso, The Effect of Magnesium Oxide Nanoparticles on the Setting Time and Properties of Glass-Ionomer Cement, *J. Int. Dental Med. Res.*, 2023, **16**(3), 1014–1021.

55 A. J. Noori and F. A. Kareem, The effect of magnesium oxide nanoparticles on the antibacterial and antibiofilm properties of glass-ionomer cement, *Heliyon*, 2019, **5**, e02568, DOI: **10.1016/j.heliyon.2019.e02568**.